Supplemental Information: The rotational spectrum of the β-cyanovinyl radical

Sommer L. Johansen, Marie-Aline Martin-Drumel, Kyle N. Crabtree

E-mail:

***cis*-β-CV rotational structure** As the cis-β-CV lines had a higher signal to noise ratio, we have focused on this species for fitting the hyperfine structure using a standard Watson A-reduced effective Hamiltonian with the coupling terms added. However, the magnitudes of the coupling terms are so similar that small changes in parameter values change the quantum numbers associated with some eigenvectors when performing a projection assignment onto the basis. In several cases, this causes two peaks separated by $\sim$100 MHz to trade quantum number assignments. Standard fitting approaches which involve minimizing the squared differences between the calculated and observed frequencies for a particular set of quantum numbers fail when sudden discontinuities like this occur. This is illustrated in Figures 2 and 1.

We attempted to circumvent this by manually modeling the spectrum, done by individually altering parameters in order to reproduce the experimental data seen in the fundamental a-type transition and in a 2D plot of the fundamental a-type versus the fundamental b-type transitions (Figure 3). The latter method in particular revealed useful patterns that helped us develop a qualitative reproduction of the spectrum. Multiple experimental a-type transitions (the "probe" lines in the double resonance experiment) were linked to the same sets of b-type transitions, which is indicative of a shared ground state between these a-type lines. This would not have been determinable without the DR linkages. Figure 4 shows our best qualitative fit. Although attempts to manually reproduce the spectrum led to new insights, the 28 term parameter space is simply too large to make a thorough model by this method.

T_1 Diagnostics and MRCI calculations In coupled cluster calculations of open shell molecules, the T_1 diagnostic is used to denote the extent of the multireference character in the electronic wavefunction. The higher the diagnostic, the greater the multireference character. Using the definition of the T_1 diagnostic from Jayatilaka and Lee[1], the results are shown in Table 1 for our CCSD(T)/ANO1 calculations. T_1 should generally be under 0.02, and our values are roughly twice this. To verify that any multireference character in

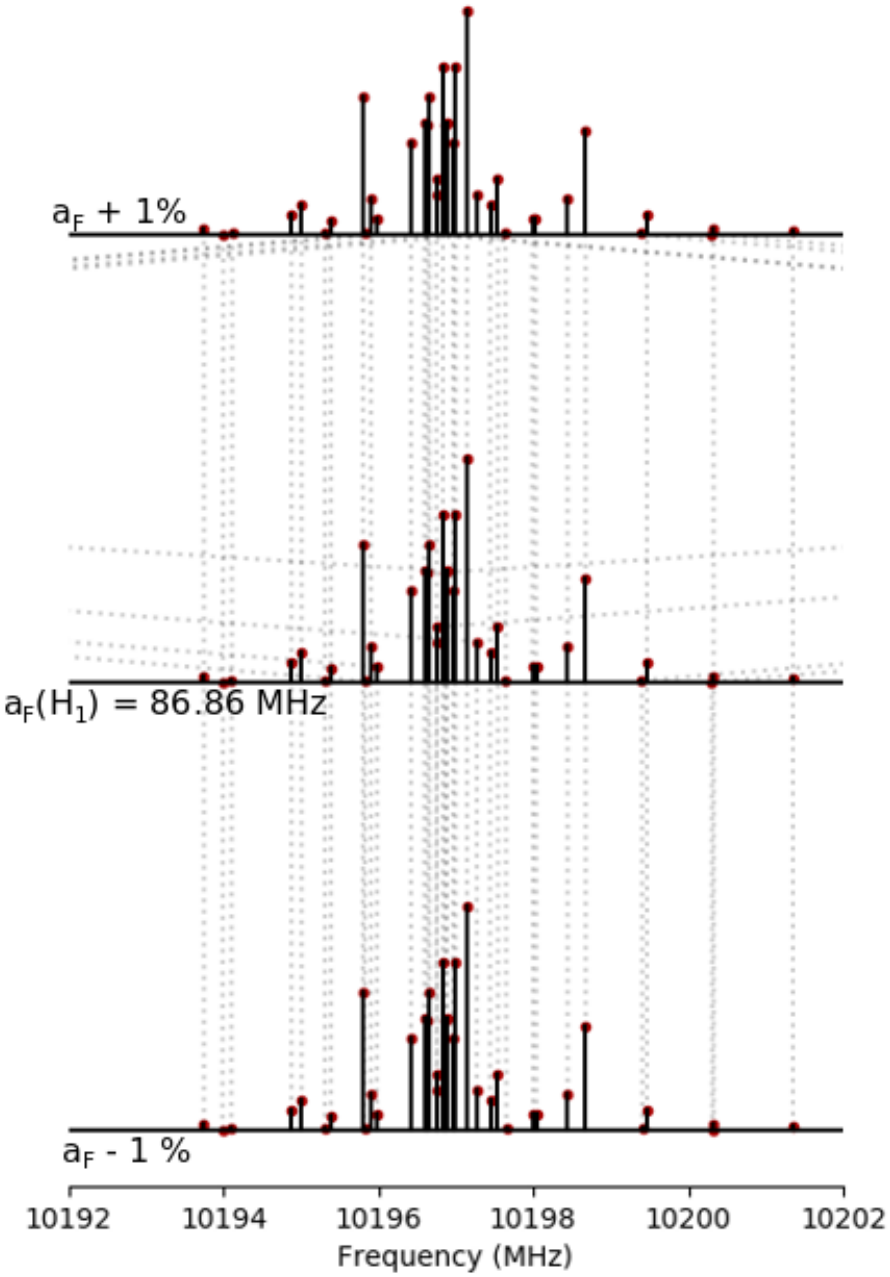

Figure 1: An illustration of the change in quantum number assignments with a small change in the value of a hydrogen Fermi contact parameter. The middle stick spectrum shows the most intense simulated lines in the $1_{01} - 0_{00}$ rotational transition of cis-β-CV. The top and bottom are the spectra with one of the hydrogen Fermi contact terms increased and decreased by 1%, respectively. Lines with identical quantum numbers are linked by dotted lines. Several lines that shift only slightly in frequency between the middle and top spectra are given different quantum number assignments, indicated by the dotted lines extending out of frame.

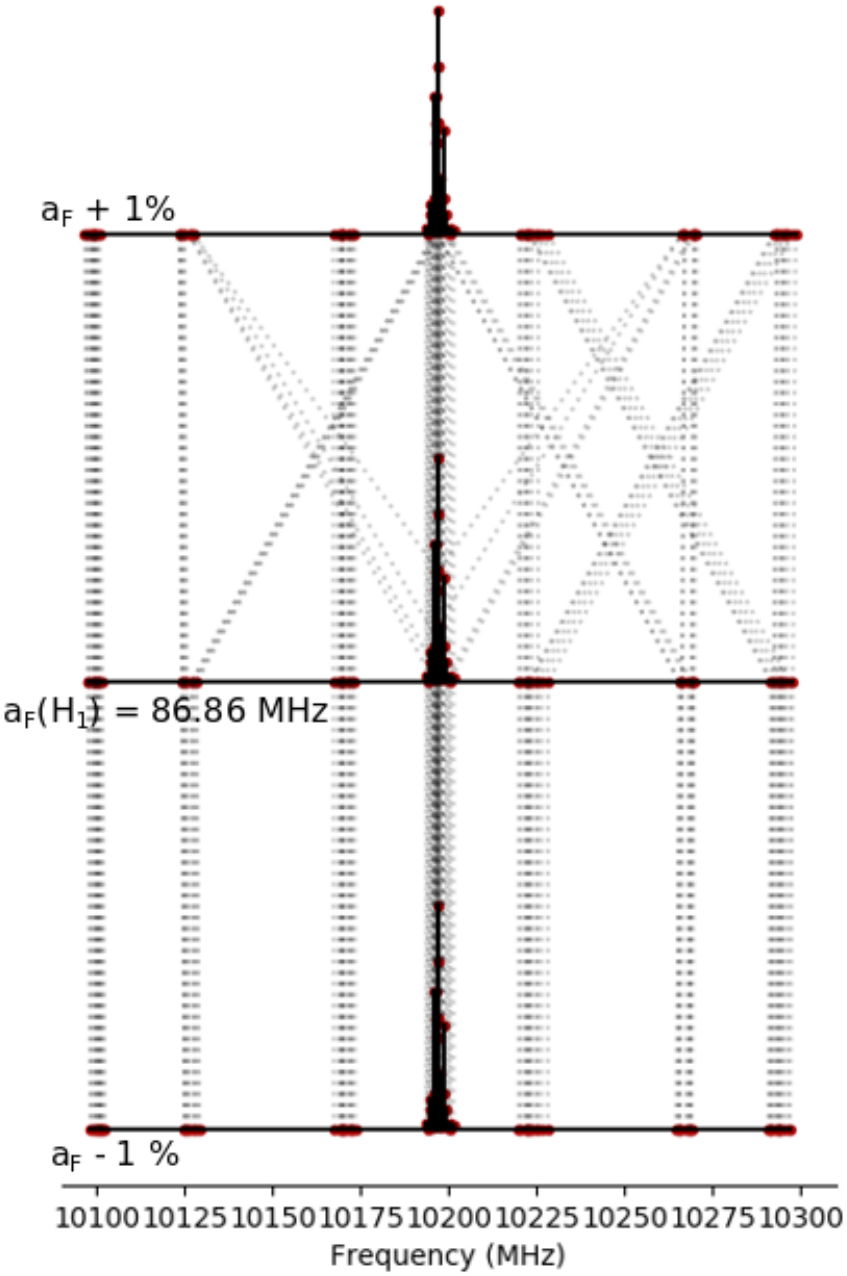

Figure 2: A zoomed-out version of Figure 1, to include every simulated component of the $1_{01} - 0_{00}$ transition in cis-β-CV.

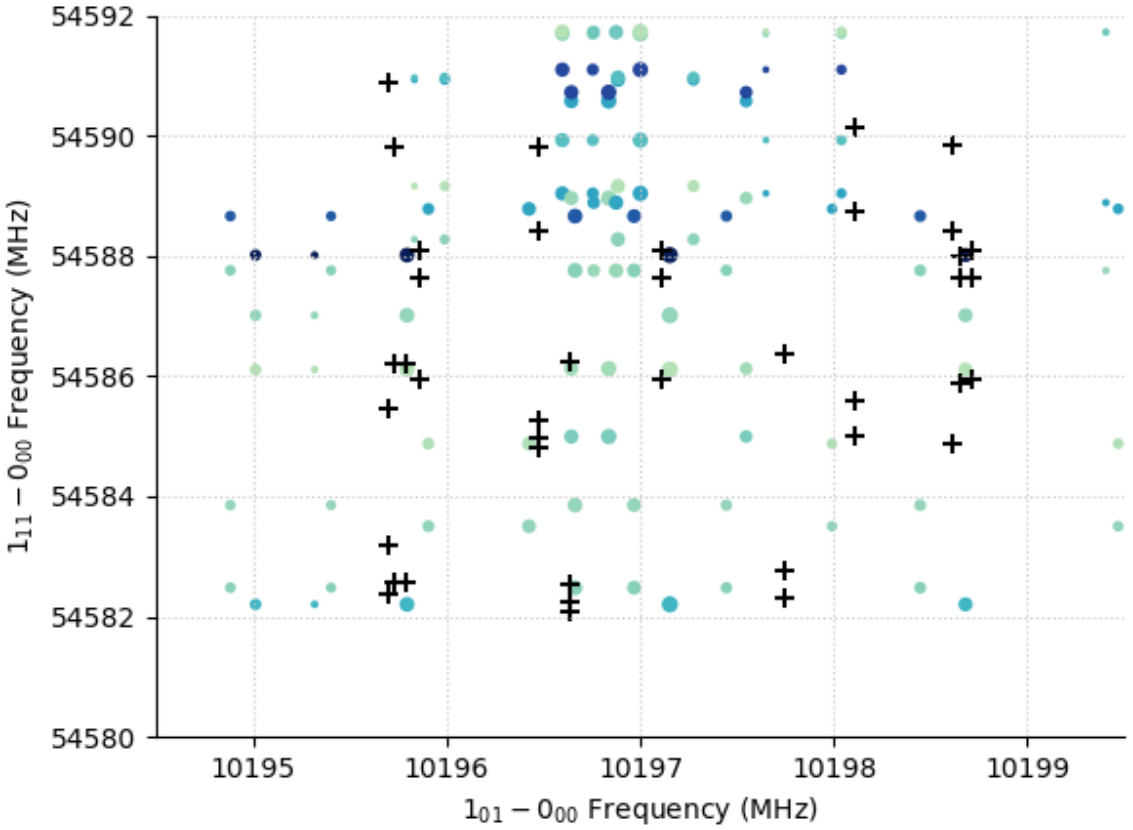

Figure 3: The 2D cis-β-CV spectrum, with experimental values labeled as black crosses and theoretical values labeled as colored dots. The frequencies of fundamental b-type transitions of cis-β-CV measured by DR are plotted along the vertical axis against their fundamental a-type monitor transition frequencies on the x axis. Sets of transition pairs that all share a common lower state are aligned vertically, while sets that share a common upper state (within $1_{11} - 0_{00}$) are aligned horizontally. The sizes of the dots are related to the calculated intensities of each $1_{01} - 0_{00}$ component, and the colors are related to the calculated intensities of each $1_{11} - 0_{00}$ component (darker colors represent stronger transitions). In an effort to fit the spectrum, parameters were varied in turn to make the simulated spectrum better match the experimental one.

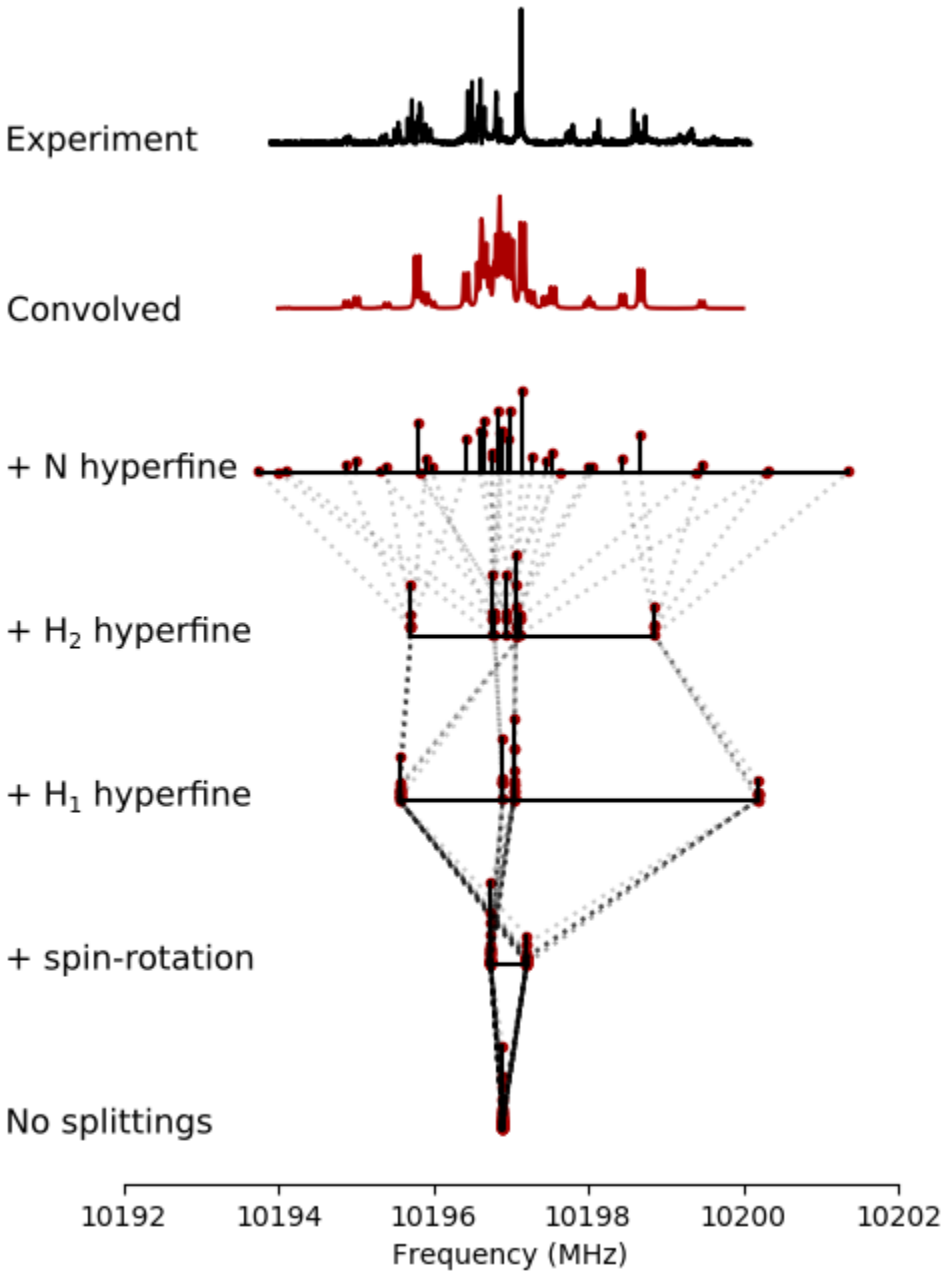

Figure 4: The cis-β-CV fundamental a-type transition, with each source of splitting added individually. From the bottom up: 1. Simple asymmetric top transition with CD terms. 2. Spin-rotation added. 3. Hydrogen 1 spin-spin added. 4. Hydrogen 2 spin-spin added. 5. N spin-spin and quadrupole added. 6. Theoretical spectrum convolved with instrumental lineshape function. 7. Experimental spectrum. This simulated spectrum reflects one of the best qualitative fits we were able to produce.

the wavefunction does not significantly affect the quality of our theoretical structures, we performed multireference configuration interaction with single and double excitations with Davidson's correction[2,3] using Dunning's augmented correlation-consistent polarized valence triple-zeta basis set[4] (MRCI+Q/aug-cc-pVTZ) as implemented in MOLPRO[5] (Table 2). All B_e and C_e values are within 1% between the two methods. The A_e values differ by about 2% for cis-β-CV and trans-β-CV, and 13.4% for α-CV. Given the smaller basis set used in the MRCI calculations, the structural agreement is satisfactory for rotational spectroscopy applications.

Table 1: T_1 Diagnostics for all CV species

Isomer	T_1 (AA)	T_1 (BB)
α-CV	0.049	0.046
cis-β-CV	0.038	0.040
trans-β-CV	0.038	0.041

Table 2: Rotational constants (in MHz) for CV isomers calculated at MRCI+Q/aug-cc-pVTZ and CCSD(T)/ANO1.

Isomer	Constant	MRCI+Q	CCSD(T)	% Diff.[a]
α-CV	A_e	152167.27	175612.55	13.4
	B_e	4456.17	4451.72	−0.1
	C_e	4329.38	4341.66	0.3
cis-β-CV	A_e	49447.10	50602.68	2.3
	B_e	5352.24	5387.26	0.7
	C_e	4829.49	4868.91	0.8
trans-β-CV	A_e	63640.54	65002.95	2.1
	B_e	5074.10	5118.28	0.9
	C_e	4699.41	4744.68	1.0

[a][CCSD(T) − MRCI+Q]/CCSD(T)

Table 3: cis-β-CV transitions measured using cavity FTMW spectroscopy, in MHz. Uncertainties on each transition are estimated to be 5 kHz.

$N'_{K'_a,K'_c} - N''_{K''_a,K''_c}$	Freq.	$N'_{K'_a,K'_c} - N''_{K''_a,K''_c}$	Freq.
$1_{01} - 0_{00}$	10194.897	$2_{02} - 1_{01}$	20389.337
$1_{01} - 0_{00}$	10195.369	$2_{02} - 1_{01}$	20389.453
$1_{01} - 0_{00}$	10195.699	$2_{02} - 1_{01}$	20389.617
$1_{01} - 0_{00}$	10195.786	$2_{02} - 1_{01}$	20389.706
$1_{01} - 0_{00}$	10195.862	$2_{02} - 1_{01}$	20389.741
$1_{01} - 0_{00}$	10195.923	$2_{02} - 1_{01}$	20389.946
$1_{01} - 0_{00}$	10196.409	$2_{02} - 1_{01}$	20390.230
$1_{01} - 0_{00}$	10196.583	$2_{02} - 1_{01}$	20390.530
$1_{01} - 0_{00}$	10196.610	$2_{02} - 1_{01}$	20390.829
$1_{01} - 0_{00}$	10196.639	$3_{03} - 2_{02}$	30569.243
$1_{01} - 0_{00}$	10196.847	$3_{03} - 2_{02}$	30569.913
$1_{01} - 0_{00}$	10197.111	$3_{03} - 2_{02}$	30570.505
$1_{01} - 0_{00}$	10197.779	$3_{03} - 2_{02}$	30570.566
$1_{01} - 0_{00}$	10198.113	$3_{03} - 2_{02}$	30570.662
$1_{01} - 0_{00}$	10198.610	$3_{03} - 2_{02}$	30571.028
$1_{01} - 0_{00}$	10198.664	$3_{03} - 2_{02}$	30571.278
$1_{01} - 0_{00}$	10198.711	$3_{03} - 2_{02}$	30571.737
$1_{01} - 0_{00}$	10199.213	$3_{03} - 2_{02}$	30571.927
$1_{01} - 0_{00}$	10199.300	$3_{03} - 2_{02}$	30572.262
$1_{01} - 0_{00}$	10199.648	$3_{03} - 2_{02}$	30572.496
$2_{12} - 1_{11}$	19862.500	$3_{03} - 2_{02}$	30572.972
$2_{02} - 1_{01}$	20387.604	$3_{03} - 2_{02}$	30573.741
$2_{02} - 1_{01}$	20387.668	$4_{04} - 3_{03}$	40738.248
$2_{02} - 1_{01}$	20388.299	$4_{04} - 3_{03}$	40738.766
$2_{02} - 1_{01}$	20388.380	$4_{04} - 3_{03}$	40738.847
$2_{02} - 1_{01}$	20388.571	$4_{04} - 3_{03}$	40739.072
$2_{02} - 1_{01}$	20388.783	$4_{04} - 3_{03}$	40739.115
$2_{02} - 1_{01}$	20388.983	$4_{04} - 3_{03}$	40739.234
$2_{02} - 1_{01}$	20389.104	$4_{04} - 3_{03}$	40739.320
$2_{02} - 1_{01}$	20389.219	$4_{04} - 3_{03}$	40742.880

Table 4: cis-β-CV transitions measured using DR, in MHz. Each transition is shown together with its linked transition measured using cavity FTMW spectroscopy. Uncertainties are in units of the last digit.

$N'_{K'_a,K'_c} - N''_{K''_a,K''_c}$(DR)	DR Freq.	$N'_{K'_a,K'_c} - N''_{K''_a,K''_c}$(Cavity)	Cavity Freq.
$1_{11} - 0_{00}$	54585.962(2.9)	$1_{01} - 0_{00}$	10197.111
$1_{11} - 0_{00}$	54587.629(2.7)	$1_{01} - 0_{00}$	10197.111
$1_{11} - 0_{00}$	54588.082(3.3)	$1_{01} - 0_{00}$	10197.111
$1_{11} - 0_{00}$	54584.800(14.6)	$1_{01} - 0_{00}$	10196.477
$1_{11} - 0_{00}$	54584.966(10.3)	$1_{01} - 0_{00}$	10196.477
$1_{11} - 0_{00}$	54585.273(4.8)	$1_{01} - 0_{00}$	10196.477
$1_{11} - 0_{00}$	54588.403(9.3)	$1_{01} - 0_{00}$	10196.477
$1_{11} - 0_{00}$	54589.820(5.2)	$1_{01} - 0_{00}$	10196.477
$1_{11} - 0_{00}$	54582.095(16.6)	$1_{01} - 0_{00}$	10196.639
$1_{11} - 0_{00}$	54582.254(7.7)	$1_{01} - 0_{00}$	10196.639
$1_{11} - 0_{00}$	54582.548(6.7)	$1_{01} - 0_{00}$	10196.639
$1_{11} - 0_{00}$	54586.225(7.2)	$1_{01} - 0_{00}$	10196.639
$1_{11} - 0_{00}$	54582.312(13.8)	$1_{01} - 0_{00}$	10197.773
$1_{11} - 0_{00}$	54582.759(9.4)	$1_{01} - 0_{00}$	10197.773
$1_{11} - 0_{00}$	54586.379(16.9)	$1_{01} - 0_{00}$	10197.773
$1_{11} - 0_{00}$	54585.018(18.0)	$1_{01} - 0_{00}$	10198.113
$1_{11} - 0_{00}$	54585.600(21.7)	$1_{01} - 0_{00}$	10198.113
$1_{11} - 0_{00}$	54588.732(15.7)	$1_{01} - 0_{00}$	10198.113
$1_{11} - 0_{00}$	54590.129(13.3)	$1_{01} - 0_{00}$	10198.113
$1_{11} - 0_{00}$	54585.974(11.7)	$1_{01} - 0_{00}$	10198.711
$1_{11} - 0_{00}$	54587.605(12.4)	$1_{01} - 0_{00}$	10198.711
$1_{11} - 0_{00}$	54588.105(14.3)	$1_{01} - 0_{00}$	10198.711
$1_{11} - 0_{00}$	54585.875(16.7)	$1_{01} - 0_{00}$	10198.653
$1_{11} - 0_{00}$	54587.623(17.2)	$1_{01} - 0_{00}$	10198.653
$1_{11} - 0_{00}$	54588.004(17.7)	$1_{01} - 0_{00}$	10198.653
$1_{11} - 0_{00}$	54584.869(48.3)	$1_{01} - 0_{00}$	10198.616
$1_{11} - 0_{00}$	54588.408(23.8)	$1_{01} - 0_{00}$	10198.616
$1_{11} - 0_{00}$	54589.839(25.6)	$1_{01} - 0_{00}$	10198.616
$1_{11} - 0_{00}$	54585.944(8.1)	$1_{01} - 0_{00}$	10195.862
$1_{11} - 0_{00}$	54587.596(6.8)	$1_{01} - 0_{00}$	10195.862
$1_{11} - 0_{00}$	54588.081(8.6)	$1_{01} - 0_{00}$	10195.862
$1_{11} - 0_{00}$	54582.559(35.7)	$1_{01} - 0_{00}$	10195.786
$1_{11} - 0_{00}$	54586.211(17.2)	$1_{01} - 0_{00}$	10195.786
$1_{11} - 0_{00}$	54582.563(14.9)	$1_{01} - 0_{00}$	10195.730
$1_{11} - 0_{00}$	54586.209(18.8)	$1_{01} - 0_{00}$	10195.730
$1_{11} - 0_{00}$	54589.802(31.8)	$1_{01} - 0_{00}$	10195.730
$1_{10} - 1_{01}$	44921.452(9.9)	$1_{01} - 0_{00}$	10197.111
$1_{10} - 1_{01}$	44922.188(5.8)	$1_{01} - 0_{00}$	10197.111
$1_{10} - 1_{01}$	44922.321(3.3)	$1_{01} - 0_{00}$	10197.111
$1_{10} - 1_{01}$	44922.906(6.5)	$1_{01} - 0_{00}$	10197.111
$2_{12} - 1_{01}$	64253.183(8.3)	$1_{01} - 0_{00}$	10197.111

Table 5: trans-β-CV transitions measured using cavity FTMW spectroscopy, in MHz. Uncertainties on each transition are estimated to be 5 kHz.

$N'_{K'_a,K'_c} - N''_{K''_a,K''_c}$	Freq.	$N'_{K'_a,K'_c} - N''_{K''_a,K''_c}$	Freq.
$1_{01} - 0_{00}$	9748.785	$2_{02} - 1_{01}$	19498.835
$1_{01} - 0_{00}$	9749.368	$2_{02} - 1_{01}$	19499.765
$1_{01} - 0_{00}$	9749.641	$2_{02} - 1_{01}$	19499.869
$1_{01} - 0_{00}$	9750.340	$2_{02} - 1_{01}$	19500.148
$1_{01} - 0_{00}$	9750.867	$2_{02} - 1_{01}$	19501.737
$1_{01} - 0_{00}$	9752.370	$2_{02} - 1_{01}$	19506.800
$1_{01} - 0_{00}$	9760.040	$2_{02} - 1_{01}$	19507.200
$1_{01} - 0_{00}$	9760.570	$3_{03} - 2_{02}$	29248.950

Table 6: trans-β-CV transitions measured using DR, in MHz. Each transition is shown together with its linked transition measured using cavity FTMW spectroscopy. Uncertainties are in units of the last digit.

$N'_{K'_a,K'_c} - N''_{K''_a,K''_c}$(DR)	DR Freq.	$N'_{K'_a,K'_c} - N''_{K''_a,K''_c}$(Cavity)	Cavity Freq.
$1_{10} - 1_{01}$	61161.701(16.4)	$2_{02} - 1_{01}$	19499.765
$1_{10} - 1_{01}$	61161.771(8.6)	$2_{02} - 1_{01}$	9750.867
$1_{10} - 1_{01}$	61161.849(26.6)	$2_{02} - 1_{01}$	19499.765
$1_{11} - 0_{00}$	70544.755(13.5)	$1_{01} - 0_{00}$	9750.867
$1_{11} - 0_{00}$	70545.547(28.5)	$1_{01} - 0_{00}$	9750.867
$1_{11} - 0_{00}$	70545.864(14.8)	$1_{01} - 0_{00}$	9750.867
$1_{11} - 0_{00}$	70699.630(6.1)	$1_{01} - 0_{00}$	9750.867
$2_{12} - 1_{01}$	79932.631(12.7)	$1_{01} - 0_{00}$	9750.867

Table 7: CCSD(T)/ANO0 harmonic and anharmonic vibrational frequencies of the cyanovinyl isomers, in cm^{-1}

	cis-β-CV		trans-β-CV		α-CV	
Mode	Harmonic	Anharmonic	Harmonic	Anharmonic	Harmonic	Anharmonic
7	223.2	223.3	235.0	235.0	176.8	163.5
8	371.1	367.5	360.5	357.7	281.2	273.3
9	529.1	524.2	550.0	545.1	468.8	452.3
10	710.9	700.8	699.3	690.5	586.1	573.4
11	855.5	819.7	797.5	773.3	853.4	830.9
12	888.5	864.7	836.6	819.9	921.8	901.9
13	984.4	948.4	1004.1	970.1	986.1	963.4
14	1263.1	1244.2	1256.4	1229.8	1426.6	1391.0
15	1643.2	1603.9	1656.4	1627.2	1764.9	1740.1
16	2371.8	2305.1	2380.1	2312.2	2172.9	2117.5
17	3197.5	3046.0	3136.7	2986.0	3122.0	2969.9
18	3274.9	3115.6	3280.1	3141.1	3227.9	3071.9
ZPVE	8156.7	8054.1	8096.4	7996.2	7994.3	7724.6

Table 8: Calculated parameters of cis- and trans-β-CV, in MHz

Parameter	cis	trans
A_0	51001.38	65143.77
B_0	5363.23	5107.83
C_0	4844.05	4728.75
$10^3\,\Delta_N$	3.13	2.15
$10^1\,\Delta_{NK}$	−41.10	−1.56
Δ_K	3.03	7.08
$10^4\,\delta_N$	6.86	4.19
$10^2\,\delta_K$	3.03	2.17
ϵ_{aa}	4.86	−99.04
ϵ_{bb}	5.82	−9.23
ϵ_{cc}	−4.77	1.66
χ_{aa}	−3.88	−4.00
χ_{bb}	1.81	1.87
χ_{cc}	2.08	2.13
χ_{ab}	1.78	1.63
a_F, N	5.03	4.07
T_{aa}, N	−1.41	−0.89
T_{bb}, N	3.00	1.45
T_{cc}, N	−1.59	−0.56
T_{ab}, N	−0.13	0.59
a_F, H_1	86.86	150.96
T_{aa}, H_1	−0.54	0.05
T_{bb}, H_1	7.28	6.25
T_{cc}, H_1	−6.74	−6.29
T_{ab}, H_1	8.93	3.28
a_F, H_2	35.33	30.31
T_{aa}, H_2	−4.57	40.86
T_{bb}, H_2	39.36	−5.71
T_{cc}, H_2	−34.79	−35.15
T_{ab}, H_2	9.26	3.44

cis-β-CV SPFIT/SPCAT input files (no splittings)

```
cis_no_spin.par
8    8   50    0     0.0000E+00     1.0000E+06    -1.0000E+00 1.0000000000
'a'     1     1   0   10  0   1   1   1   0   0   1
10000   4.975753840412576E+04 1.00000000E+36
20000   5.364295487047583E+03 1.00000000E+36
30000   4.832548502995252E+03 1.00000000E+36
299    -3.129900000000000E-03 1.38789580E-37 /-Delta_N
2099   -3.025700000000001E+00 1.38789580E-37 /-Delta_K
1199    1.101800000000000E-01 1.38789580E-37 /-Delta_NK
40199  -6.863400000000001E-04 1.38789580E-37 /-delta_J
41099  -3.032420000000000E-02 1.38789580E-37 /-delta_K

cis_no_spin.lin
1  0  1  0  0  0                      10196.6680     0.6000  2.481E-07
2  0  2  1  0  1                      20389.1791     0.6000  1.648E-06
1  1  1  0  0  0                      54586.1531     2.4000  1.517E-05
1  1  0  1  0  1                      44922.1790     0.6000  1.500E-05
2  1  2  1  0  1                      64253.1830     2.4000  1.500E-05
3  0  3  2  0  2                      30571.4100     0.6000  1.500E-05
4  0  4  3  0  3                      40738.8600     0.6000  1.500E-05
2  1  2  1  1  1                      19862.5000     0.6000  1.000E-05

cis_no_spin.int
112     1 1314.0  0  10      -50. -50.  95.00
1     3.00
2     0.45
```

cis-β-CV SPFIT/SPCAT input (ab initio)

```
cis_theory.par
28    4   10    2     0.0000E+00     1.0000E+06    -1.0000E+00 1.0000000000
'a'  3222  1   0  9   0  1   1   1   1   -1   1
10000      5.100137806000000E+04 1.00000000E-37
20000      5.363234180000000E+03 1.00000000E-37
30000      4.844050234000000E+03 1.00000000E-37
299       -3.129900000000000E-03 1.38789580E-37 /-Delta_N
2099      -3.025700000000001E+00 1.38789580E-37 /-Delta_K
1199       1.101800000000000E-01 1.38789580E-37 /-Delta_NK
40199     -6.863400000000001E-04 1.38789580E-37 /-delta_J
41099     -3.032420000000000E-02 1.38789580E-37 /-delta_K
10010099   4.860147000000000E+00 1.38789580E-36 /e_aa
10020099   5.824045000000000E-00 1.59003886E-37 /e_bb
10030099  -4.771722000000000E-00 1.00000000E-37 /e_cc
440010099 -5.824115625000000E+00 5.69881433E-37 /3chi.aa/2
440040099 -6.768278000000000E-02 1.38789580E-37 /chi(b-c)/4
440610099  1.778292100000000E+00 1.00000000E-37 /chi.ab
140000099  5.032457602313510E+00 1.38789580E-37 /a_f
140010099 -2.116078535548397E+00 1.00000000E-37 /1.5 T_aa
140040099  1.147461860475000E+00 1.38789580E-37 /T_(bb-cc)/
140610099 -1.335385985000000E-01 1.00000000E-37 /T.ab
130000099  8.686288970506232E+01 1.38789580E-37 /a_f
130010099 -8.030599569565532E-01 1.00000000E-37 /1.5 T_aa
130040099  3.505340275800000E+00 1.38789580E-37 /T_(bb-cc)/
130610099  8.928931614000000E+00 1.00000000E-37 /T.ab
120000099  3.532996519467918E+01 1.38789580E-37 /a_f
120010099 -6.860313681454295E+00 1.00000000E-37 /1.5 T_aa
120040099  1.853906216962000E+01 1.38789580E-37 /T_(bb-cc)/
120610099  9.259691231000000E+00 1.00000000E-37 /T.ab
```

trans-β-CV SPFIT/SPCAT input files (spin-rotation splitting only)

```
trans_spin_rot_only.par
11    9   10    2     0.0000E+00     1.0000E+06    -1.0000E+00 1.0000000000
'a'  2  1   0  9   0  1   1   1   1   -1   0
10099      6.591832899532368E+04 1.00000000E-37 /A
20099      5.068497891984823E+03 1.00000000E-37 /B
30099      4.684555696741106E+03 1.00000000E-37 /C
299       -2.150000000000000E-03 1.00000000E-37 /-Delta_N
1199       1.560000000000006E-01 1.00000000E-37 /-Delta_NK
2099      -7.080000000000000E+00 1.00000000E-37 /-Delta_K
40199     -4.190000000000000E-04 1.00000000E-37 /-delta_J
41099     -2.170000000000000E-02 1.00000000E-37 /-delta_K
10010099  -2.099057158368144E+02 1.00000000E-37 /e_aa
10020099  -1.736750179679782E+01 1.00000000E-37 /e_bb
-10030099  3.123516032793540E+00 1.00000000E-37 /e_cc

trans_spin_rot_only.lin
1  0  1  2  0  0  0  1              9750.2285     1.6500  6.494E-05
1  0  1  1  0  0  0  1              9760.1000     1.6500  4.195E-05
2  0  2  3  1  0  1  2             19500.0023     1.6500  3.000E-05
2  0  2  2  1  0  1  1             19507.0000     1.6500  1.000E-05
1  1  1  2  0  0  0  1             70545.3887     1.8050  2.874E-04
1  1  1  1  0  0  0  1             70699.6250     1.8050  2.874E-04
1  1  0  2  1  0  1  1             61161.9450     1.8050  1.200E-04
3  0  3  4  2  0  2  3             29248.9500     1.6500  1.500E-04
2  1  2  3  1  0  1  2             79932.6300     1.8050  1.500E-04

trans_spin_rot_only.int
0  1  13387.5632  0  9  -15.2 -9.0 4444.0 5
1  3.00
2  1.00
```

trans-β-CV SPFIT/SPCAT input (ab initio)

```
trans_theory.par
22   32   10    2     0.0000E+00     1.0000E+06     -1.0000E+00 1.0000000000
'a'  3222  1   0  9   0  1   1   1   1   -1   0
10099       6.5143772700000000E+04 1.00000000E-37 /A
20099       5.1078287000000000E+03 1.00000000E-37 /B
30099       4.7287465000000000E+03 1.00000000E-37 /C
299        -2.1500000000000000E-03 1.00000000E-37 /-Delta_N
1199        1.5600000000000000E-01 1.00000000E-37 /-Delta_NK
2099       -7.0800000000000000E+00 1.00000000E-37 /-Delta_K
40199       4.1900000000000000E-04 1.00000000E-37 /-delta_J
41099       2.1700000000000000E-00 1.00000000E-37 /-delta_K
10010099   -9.9043286000000000E+01 1.00000000E-37 /e_aa
10020099   -9.2317900000000000E+00 1.00000000E-37 /e_bb
10030099    1.6648320000000000E+01 1.00000000E-37 /e_cc
440010099  -6.0039178050000000E+00 1.00000000E-37 /3chi.aa/2
440040099  -6.3955000000000000E-02 1.00000000E-37 /chi(b-c)/4
140000099   4.0662708193000000E+00 1.00000000E-37 /a_f
140010099  -1.3370307292500000E+00 1.00000000E-37 /1.5 T_aa
140061099   0.5963297482000000E+00 1.00000000E-37 /T_ab
140040099   0.5042080676750000E+00 1.00000000E-37 /T_(bb-cc)/4
130000099   1.5095903096650000E+02 1.00000000E-37 /a_f
130010099   0.0678904075500000E+00 1.00000000E-37 /1.5 T_aa
130061099   3.2803519551000000E+00 1.00000000E-37 /T_ab
130040099   3.2289820678200000E+00 1.00000000E-37 /T_(bb-cc)/4
120000099   3.0311775313800000E+00 1.00000000E-37 /a_f
120010099   6.1296848465750000E+00 1.00000000E-37 /1.5 T_aa
120061099   3.4520019980000000E+00 1.00000000E-37 /T_ab
120040099   7.3603246580000000E+00 1.00000000E-37 /T_(bb-cc)/4
```

References

(1) Jayatilaka, D.; Lee, T. J. Open-shell coupled-cluster theory. *The Journal of Chemical Physics* **1993**, *98*, 9734–9747.

(2) Werner, H.; Knowles, P. J. An efficient internally contracted multiconfiguration–reference configuration interaction method. *The Journal of Chemical Physics* **1988**, *89*, 5803–5814.

(3) Langhoff, S. R.; Davidson, E. R. Configuration interaction calculations on the nitrogen molecule. *International Journal of Quantum Chemistry* **1974**, *8*, 61–72.

(4) Kendall, R. A.; Dunning, T. H.; Harrison, R. J. Electron affinites of the first-row atoms

revisited. Systematic basis sets and wave functions. *The Journal of Chemical Physics* **1992**, *96*, 6796.

(5) Werner, H.; Knowles, P.; Knizia, G.; Manby, F.; Schütz, M.; Celani, P.; Györffy, W.; Kats, D.; Korona, T.; Lindh, R. et al. MOLPRO, version 2015.1, a package of ab initio programs. *University of Cardiff Chemistry Consultants (UC3): Cardiff, Wales, UK* **2015**,